Predicted fire behaviour of steels and concrete structures

Anderberg, Yngve

1983

LUND INSTITUTE OF TECHNOLOGY · LUND · SWEDEN
DIVISION OF BUILDING FIRE SAFETY AND TECHNOLOGY
REPORT LUTVDG/(TVBB - 3011)

YNGVE ANDERBERG

PREDICTED FIRE BEHAVIOUR OF STEELS AND CONCRETE STRUCTURES

LUND 1983

PREDICTED FIRE BEHAVIOUR OF STEELS AND CONCRETE STRUCTURES

by Yngve Anderberg, Dr Techn

Division of Building Fire Safety and Technology, Lund Institute of Technology, Sweden

---

ABSTRACT

Analytical modelling has opened the door for fire behaviour prediction of not only building materials as concrete and steel but also of quite complicated concrete structures in general. This paper reflects some of the progress made within this field.

A behaviour model of steel is used for coupling results from steady state and transient state tests. A recently developed procedure is shown on how to interpret and make such results comparable for practical use.

The computational capability and reliability are illustrated for TASEF-2 temperature program and CONFIRE structural program developed at Lund Institute of Technology (LTH), Sweden and Norwegian Institute of Technology (NTH), Norway, respectively. The success of computation is decisively dependent on reliable material models. The influence of axial restraint on failure time is exemplified.

1 MATERIAL BEHAVIOUR MODELS

1.1 Concrete

When modelling material mechanical behaviour, an analytical description is required of the relationship between stresses and strains. A computer oriented constitutive model for concrete in compression, valid at transient high temperature conditions, was presented in Anderber & Thelandersson (1976) [1] and is used here in the structural program CONFIRE [2]. The model is based on the concept that the total strain ε can be separated into four components

$$\varepsilon = \varepsilon_{th}(T) + \varepsilon_{\sigma}(\bar{\sigma},\sigma,T) + \varepsilon_{cr}(\sigma,T,t) + \varepsilon_{tr}(\sigma,T) \qquad (1)$$

where

ε_{th} = thermal strain, including shrinkage, measured on specimens under variable temperature,

ε_{σ} = instantaneous, stress-related strain, based on stress-strain relations obtained under constant, stabilized temperature

ε_{cr} = creep strain or time-dependent strain measured under constant stress and stabilized temperature

ε_{tr} = transient strain, accounting for the effect of temperature increase under stress, derived from tests under constant stress and variable temperature

σ = stress

$\bar{\sigma}$ = stress history

T = temperature

t = time.

The order of importance for the strain components can be studied from Fig. 1 which is based on a curve representing a transient test with a load level of 35% of initial ultimate load. The predominance of the transient strain is obvious.

A complete description of the model is given in [1].

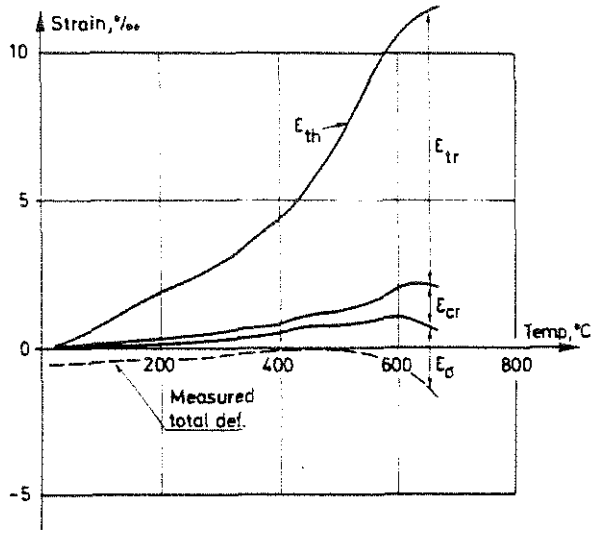

Fig. 1 Relation between different strain components as calculated by the material model for a transient test at a load level of 35% of ultimate load at ambient conditions

1.2 Steel

It is generally agreed that the deformation process of steel at transient high temperatures can be described by three strain components defined by the constitutive equation

$$\varepsilon = \varepsilon_{th}(T) + \varepsilon_{\sigma}(\sigma,T) + \varepsilon_{cr}(\sigma,T,t) \qquad (2)$$

where

ε_{th} = thermal strain

ε_{σ} = instantaneous, stress-related strain based on stress-strain relations obtained under constant, stabilized temperature

ε_{cr} = creep strain or time dependent strain.

A computer oriented mechanical behaviour model for steel, based on Eq. (2), is developed in Anderberg (1976) [3] and applied in CONFIRE.

The strains are found separately in different steady state tests. It is shown that a behaviour model based on steady state data satisfactorily predicts behaviour in transient tests under any given fire process, load and strain history.

An analytical description of the σ-ε curve as a function of temperature can be made in different ways as illustrated in Figs. 2 and 3. In the first case the curve is approximated by two straight lines (used in CONFIRE) and in the second case by an elliptic branch placed between straight lines (used in chapter 2).

Models of creep are in most cases based on a concept put forward by Dorn (1954) [4], in which the effect of variable temperatures is considered. The extension of the model to be applicable to variable stress can, for instance, be based on the strain hardening rule.

The creep strain is assumed to be dependent on the magnitude of stress and on the temperature-compensated time evaluated from the expression

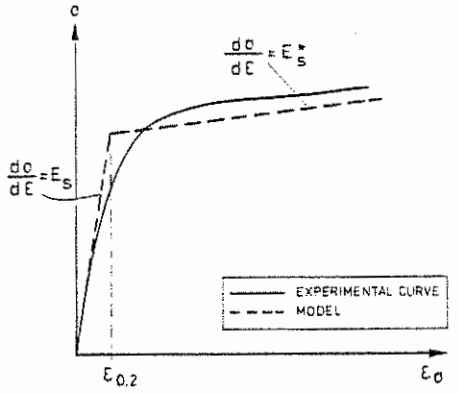

Fig. 2 Simplified model of the stress-strain curve for steel (used in CONFIRE)

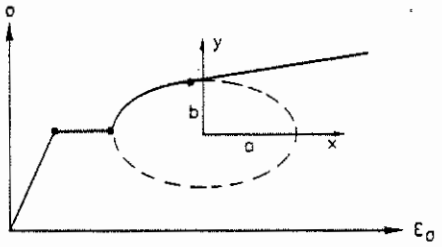

Fig. 3 Refined model of stress-strain curve for steel (used in chapter 2)

$$\Theta = \int_0^t e^{-\frac{\Delta H}{RT}} dt \quad (h) \qquad (3)$$

where
ΔH = activation energy of creep, J/mol
R = gas constant, J/mol·K
t = time.

The relation between creep strain, ε_{cr}, and temperature-compensated time, Θ, at different stress levels is shown principally in Fig. 4.

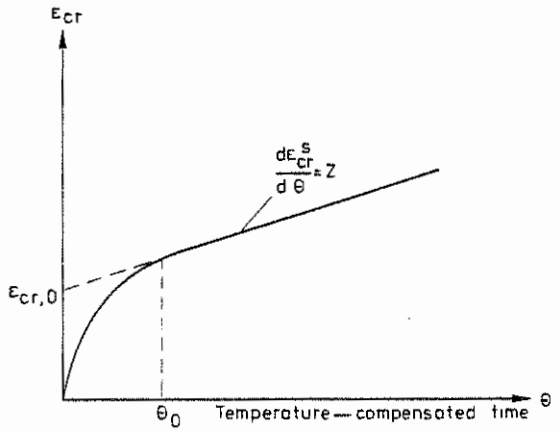

Fig. 4 Principal creep curve for the steel according to Dorn's theory

The change from the curved branch to the straight line (primary and secondary phase) is denoted Θ_o and the intersection between the straight line and the creep axis is called $\varepsilon_{cr,o}$. The slope of the straight line is called $\not{\varepsilon}$. The primary phase is defined by a parabolic equation and the secondary phase by a linear slope. The transfer occurs at time Θ_o. The mathematical formula is

$$\left.\begin{aligned} \varepsilon_{cr} &= \varepsilon_{cr,o}\left(2\sqrt{\frac{Z \cdot \Theta}{\varepsilon_{cr,o}}}\right) \quad \text{when } 0 \le \Theta \le \Theta_o \\ \varepsilon_{cr} &= \varepsilon_{cr,o}\left(1+\frac{Z \cdot \Theta}{\varepsilon_{cr,o}}\right) \quad \text{when } \Theta \ge \Theta_o \end{aligned}\right\} \qquad (4)$$

where

$$\Theta_o = \frac{\varepsilon_{cr,o}}{Z} \qquad (5)$$

Using the complete behaviour model as expressed above, any test can be simulated. The total deformation as a function of temperature measured in a transient test, $\dot{T} = 10^{o}C/min$, is calculated and the comparison is illustrated in Fig. 5.

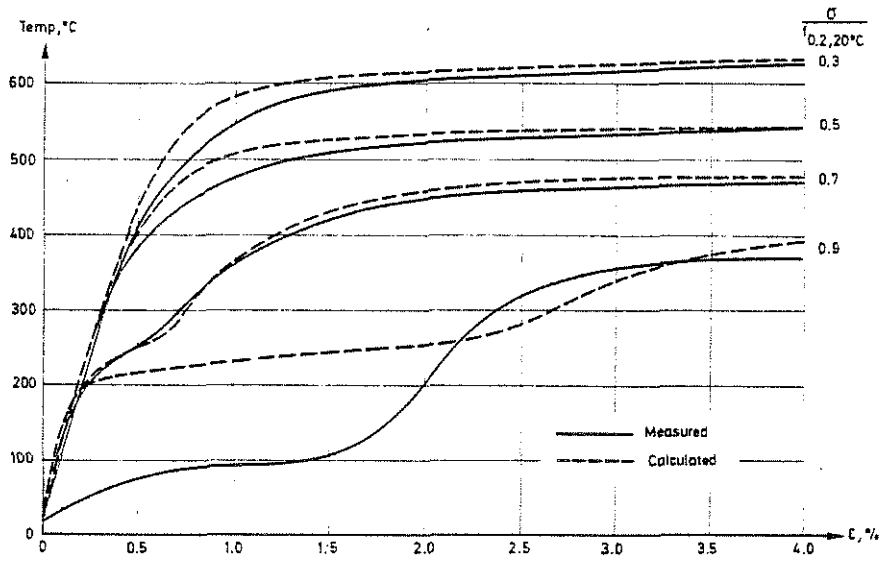

Fig. 5 Measured and predicted total deformation as a function of temperature at different load levels in a transient process, $\dot{T} = 10^{o}C/min$. Reinforcing steel Ks 60 Ø8, $f_{0.2,20^{o}C} = 710$ MPa, Anderberg (1978) [5]

It is also possible to simulate a relaxation test. A comparison is made in Fig. 6 between measured and predicted curves for reinforcing steel, Ks 60. The agreement is satisfactory.

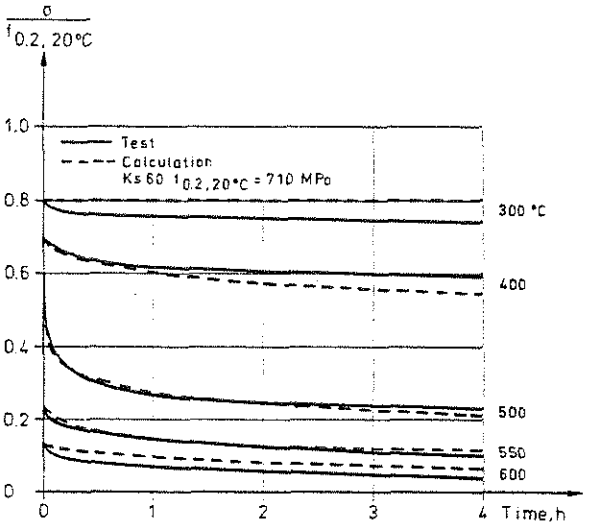

Fig. 6 Measured and predicted relaxation curves for reinforcing steel

2 A PROCEDURE TO INTERPRET AND COMPARE TEST RESULTS

2.1 Different test methods

There exist two main groups of tests, steady state tests and transient state tests. Material properties measured are closely related to the test method used. It is therefore of great importance that the test conditions are well defined.

During a fire situation the material is normally subjected to transient processes with varying temperature and stress, and to understand this, transient state tests are needed.

Mechanical properties of steel can be established by following a number of different test procedures. The three main test parameters are the heating process, application and control of load, and control of strain. These can have constant values or be varied during testing, giving steady state or transient state conditions depending on the heating procedure.

Six practical regimes which can be used for determining mechanical properties are illustrated in Fig. 7. Properties in these regimes are as follows:

steady state tests

- stress-strain relationship (stress rate control)
- stress-strain relationship (strain rate control)
- creep
- relaxation

transient state tests

- failure temperature, total deformation (stress control)
- restraint forces, total forces (strain control)

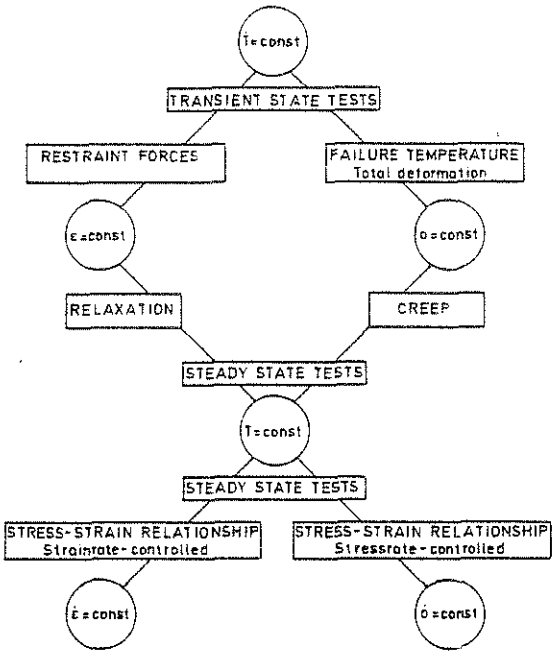

Fig. 7 Different testing regimes for determining mechanical properties RILEM PHT-44 (1982) [6]

2.2 Coupling of steady state and transient state results

Analytical modelling illustrated above makes it possible to couple steady state tests and transient state tests. For instance, the strain or stress rate can be determined in steady state tests to give the same ultimate strength as occurs in a transient test for a given rate of heating.

The predicted influence of stress and strain rates on the stress-strain relationship under steady state conditions can be studied in Figs. 8-10. From such curves the ultimate strength as a function of temperature can be evaluated. In Fig. 11 a-b, the influence of stress and strain rates on the ultimate strength under steady state conditions is illustrated. The influence of rate of temperature under transient state conditions is given in Fig. 11 c. The ultimate strength is defined by the stress at which the strain is 4%, the thermal strain excluded.

In the analytical modelling the strain and stress rate in a steady state procedure to give the same ultimate strength as under transient state conditions is found, if the rate of heating is chosen to be 10°C/min. The result is shown in Fig. 11 d for a specific reinforcing steel (Ks 60, $f_{0.2,20°C} = 710$ MPa). The strain and stress rates obtained by computation are thus

$$\dot{\varepsilon} = 20‰/\text{min}$$

and

$$\dot{\sigma} = 0.20 \text{ MPa/s} = 12 \text{ MPa/min}$$

These values vary somewhat depending on the type of steel, which is shown in Table 1 for,

a) structural steel 1411, $f_{0.2,20°C} = 340$ MPa

b) hot-rolled reinforcing steel Ks 40, $f_{0.2,20^\circ C} = 456$ MPa

c) hot-rolled reinforcing steel Ks 60, $f_{0.2,20^\circ C} = 710$ MPa

d) prestressing steel ASTM A 421-65, $f_{0.2,20^\circ C} = 1470$ MPa

Table 1

Type of steel	$\dot{T}$ °C/min	$\dot{\sigma}$ MPa/s	$\dot{\varepsilon}$ ‰/min
Steel 1411	10	0.20	10
Ks 40	10	0.20	10
Ks 60	10	0.20	20
ASTM A 421-65	10	0.50	10

For the additional steels in Table 1 the results of computation are given in Appendix.

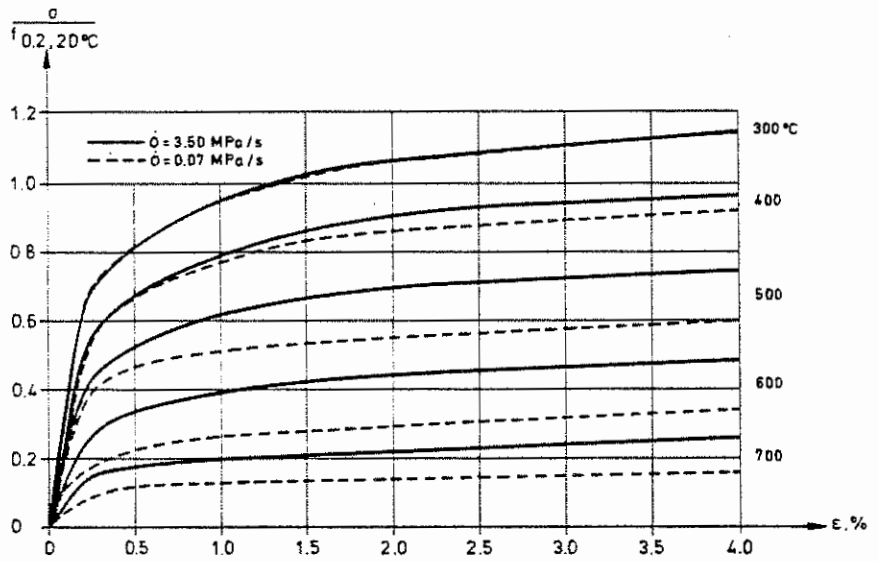

Fig. 8 Predicted σ-ε curves at different stress rates for reinforcing steel (Ks 60, $f_{0.2,20^\circ C} = 710$ MPa)

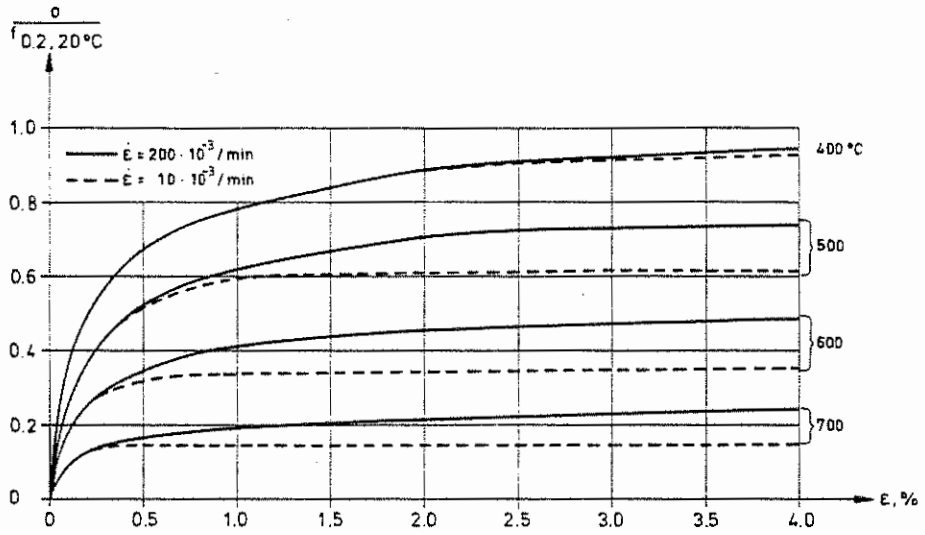

Fig. 9 Predicted σ-ε curves at different strain rates for reinforcing steel (Ks 60, $f_{0.2,20^\circ C} = 710$ MPa)

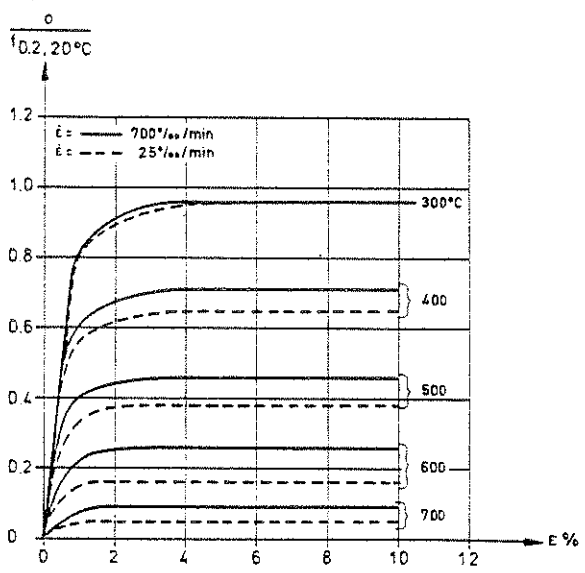

Fig. 10 Predicted σ-ε curves at different strain rates for prestressing steel (ASTM A 421-65, $f_{0.2,20°C} = 1470$ MPa)

If the strength-temperature curve, based on the transient state condition where for instance $\dot{T} = 10°C/min$ is accepted as a reference curve, test results can be directly interpreted and, thus, comparable. If the rates $\dot{\varepsilon}$ and $\dot{\sigma}$ are below the values mentioned above, the measured ultimate strength should be corrected upwards. If one has the opposite situation the strength values are corrected downwards.

The rate of stress or strain in a steady state test and the rate of temperature in a transient test are governing the development of creep which causes the change in the ultimate strength. The influence of creep for three different procedures is also fully illustrated in

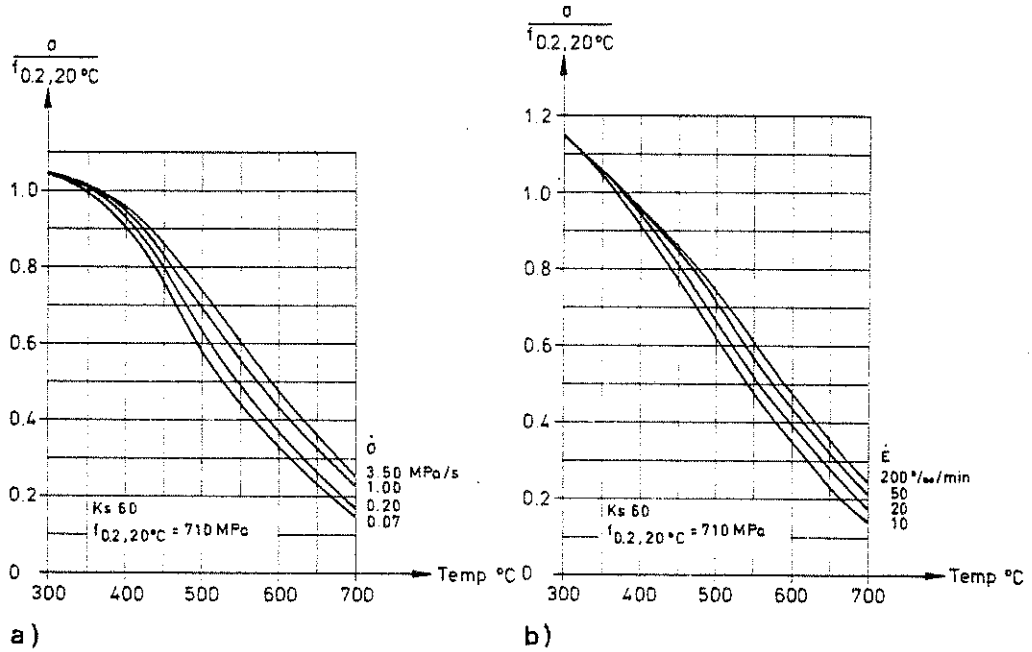

Fig. 11 Predicted ultimate strength versus temperature for reinforcing steel
a) steady state, stressrate controlled
b) steady state, strainrate controlled

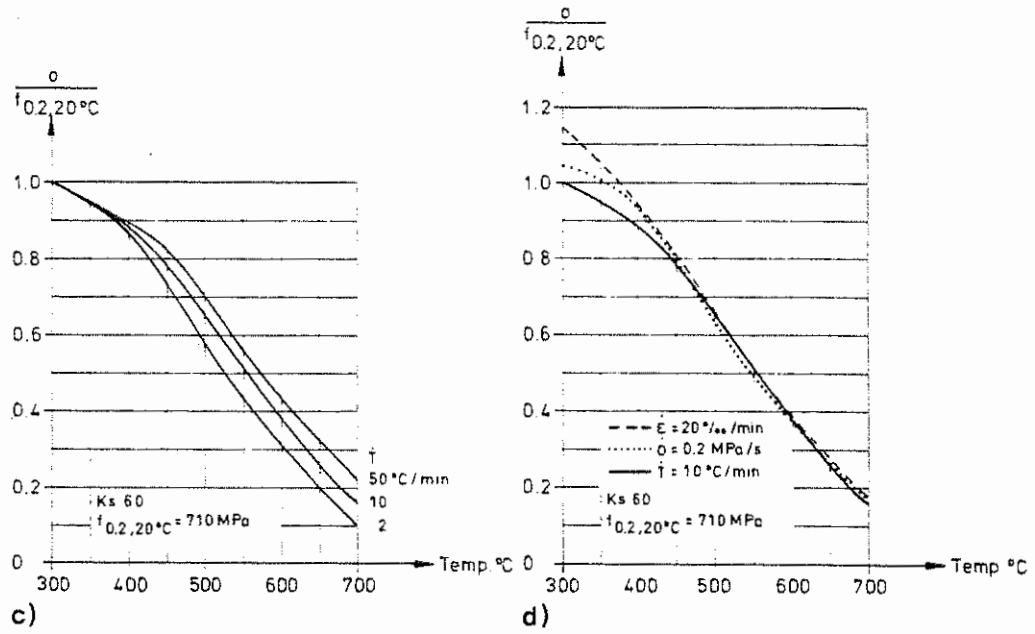

Fig. 11 Predicted ultimate strength versus temperature for reinforcing steel Ks60
c) transient state
d) comparison between steady state and transient state

Figs. 8-10. It is also important to observe that there is a great difference between the time history of creep development in a stress and strain controlled steady state test. This is principally illustrated in Fig. 12, where curve 1 represents a stress-strain curve at a very high stress or strain rate and curves 2 and 2' represent a curve at a slow stress and strain rate, respectively. The points A and A' indicate the time at which creep starts to be significant and

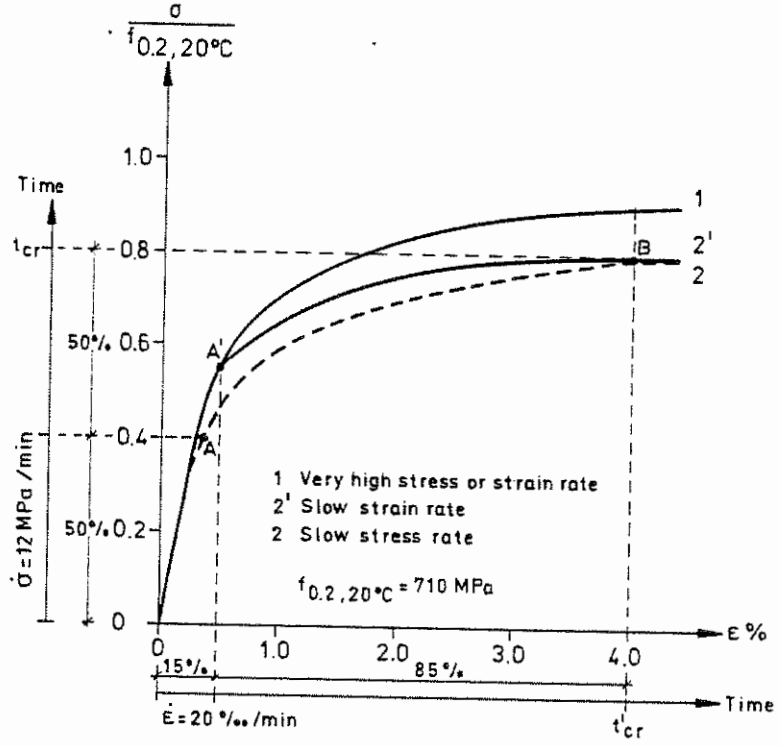

Fig. 12 Principal σ-ε curves in stress and strain controlled steady state tests with time scales indicated (t'_{cr} and t_{cr} represent the testing period)

point B is the assumed failure point ($\varepsilon = 4\%$). In the stress controlled test the time to reach point A is about 50% of the total testing period but in the strain controlled test the corresponding time is only about 15%. If a test is carried out at 600°C at the stress rate $\dot{\sigma} = 12$ MPa/min and at the strain rate $\dot{\varepsilon} = 20‰/\text{min}$ the testing period amounts to 22 and 2 min, respectively. Although these differences exist, the creep influence on the ultimate strength is the same. In the corresponding transient test this period is about 58 min. This means that the testing period is not a critical parameter in the analytical study but rather the time period of the test when creep develops.

2.3 Practical use for design

In fire-exposed concrete structures the temperature rise or rate of increase for the steel is dependent on two main factors, namely, the location of the steel (distance to exposed surfaces) and the fire curve. When the concrete cover is about 2-3 cm and the fire is characterized by the standard curve ISO 834 the rate of temperature increase does not reach more than 10°C/min. In normal cases the rate of heating for the steel is about 4-10°C/min. The rate of heating at different depths, for instance, 2 and 4 cm for a fire exposure according to ISO 834 can be studied in Fig. 20. The rate of heating varies with time and in a theoretical classification for 60 and 120 min fire duration the rate of heating for the steel is different and ought to be considered. When hot-rolled steel is used the creep is negligible at temperatures below 400°C and for prestressing steel the limit is 250°C.

The principal procedure for determining the relevant rate of heating at a depth of 2 cm for hot-rolled and cold-drawn steel at 60 min fire duration is illustrated in Fig. 13. The rate of heating for prestressing steel is determined from the branch 1-1' and for hot-rolled steel from the branch 2-2' of the curve. The rate of heating influences the ultimate strength and, thus, the design strength. The design strength can be found in Fig. 11 or Figs. A1-A3 in Appendix by maximum temperature and rate of heating as input. If one assumes that the strength is obtained from a steady state test (strain controlled $\dot{\varepsilon} = 200‰/\text{min}$, Fig. 11 b) and the design temperature is for example 550°C and the rate of heating 10°C/min, how is the design strength determined? The procedure is shown below:

$T = 550°C$, $\dot{\varepsilon} = 200‰/\text{min}$ } Fig. 11 b $\Rightarrow k = \sigma/f_{0.2,20°C} = 0.61$

$\dot{T} = 10°C/\text{min}$ Fig. 11 d $\Rightarrow$ comparable strain rate $\dot{\varepsilon} = 20‰/\text{min}$

The design strength is determined for $\dot{\varepsilon} = 20‰/\text{min}$ in Fig. 11 d and k is reduced to 0.52.

If for instance $\dot{T} = 2\ °C/\text{min}$ the design strength is obtained from Fig. 11 c and k is reduced to 0.44.

The procedure presented above gives the designer a rational way to find the fire design strength of steel even if strength characteristics only are related to steady state conditions. This coupling of steady state and transient state results makes direct comparisons possible at quite different test conditions.

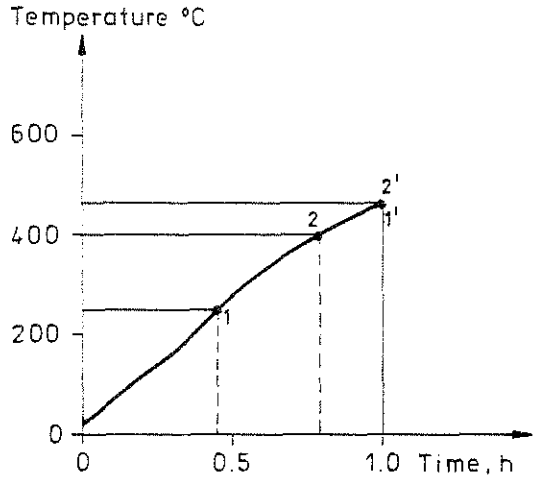

Fig. 13 Time period under which rate of heating is determined for 1-1' prestressing steel and for 2-2' hot-rolled steel at a depth of 2 cm and a standard fire duration of 1 hour

3 FIRE RESPONSE OF CONCRETE STRUCTURES

The first well-known approach using computer related discretization techniques in analysing reinforced concrete frames in fires (FIRES-RC) was published in 1974 by Becker and Bresler [7]. A revised version of the analytical method was presented in 1977 [8]. In 1976 Anderberg [9] established a special version of the computer program FIRES-RC. This version included new material behaviour models developed at the Lund Institute of Technology in Sweden [1], [3].

Geometrical non-linearities were first considered by Haksever (1977) in analysing fire-exposed slender L-frames. In 1982 both geometrical non-linearities and material models described in chapter 1 was considered by Forsén [2] in the Finite Element Program CONFIRE.

3.1 Computer programs

Three computer programs, based on the Finite Element Method, are employed in the numerical examples presented in the subsequent sections:

- TASEF-2 by Wickström [10] for the non-linear transient heat flow analysis,
- FIRES-RC by Becker & Bresler [7] in a modified version presented by Anderberg [3] for the non-linear analysis of concrete frames subjected to fire
- CONFIRE by Forsén [2] for the non-linear analysis of concrete frames subjected to fire.

TASEF-2 is developed from the Fourier heat balance equation in matrix form for a two dimensional field. Rectangular and/or triangular elements may be employed. The temperature dependent conductivity coefficient and specific volumetric enthalpy are given as input.

An arbitrary external termperature-time curve, which may be defined by the user, simulates the fire exposure. The temperature distribution within the structure at prescribed times are obtained by use of an explicit forward integration method.

FIRES-RC is originally constructed at UCB in California, but this version can be characterized as an extension of the Berkeley program. The program is based on a non-linear direct stiffness formulation

coupled with a time-step integration. Geometrical non-linearities are not considered.

CONFIRE is developed from the computer program CONFRAME by Åldstedt [11]. A beam element with 3 degrees of freedom (DOF) at each node and one internal axial DOF is employed. The total strain ε over the cross-section of the element is taken as linear (Bernoulli-Navier). The temperature related material behaviour models for steel and concrete defined in section 1 are incorporated. The linear geometric effects may also be accounted for. The linear element tangent stiffness matrixes and the element stress resultant vectors are obtained by Gaussian integration with fixed integration points. The geometric element stiffness matrix is obtained by analytical integration. The time dependent stresses, strains and structural displacements are obtained step by step by use of the Newton-Raphson iteration method, solving the linearized incremental system equilibrium equation. The current temperature distributions are recorded at each step from a temperature file.

3.2 Fire-exposed plate strips

3.2.1 Simply supported

The structural response of a simply supported, fire-exposed plate strip is predicted by use of TASEF-2 [4] and CONFIRE [2]. The fire exposure is given by the standard temperature-time curve according to the ISO 834 fire resistance test. Three different cases are considered [13], see Fig. 14

- Case 1 : Reinforced plate strip, twin load 13.8 kN (65% of initial ultimate load)
- Case P1: Prestressed plate strip, twin load 13.8 kN (65% of initial ultimate load and initial prestressing strain = 5‰)
- Case P2: Prestressed plate strip, twin load 10 kN (full prestressing at the time t = 0 and initial prestressing strain = 5‰)

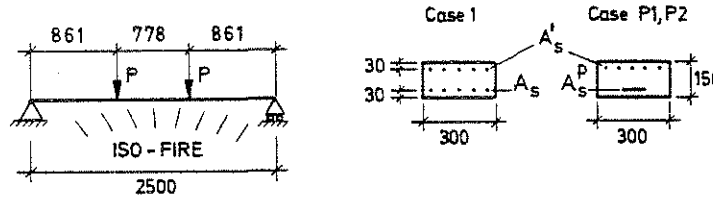

$$A_s = 391 \text{ mm}^2 \quad A_s^P = \frac{450}{1450} \cdot 391 = 121 \text{ mm}^2$$

f_{cc} = 20 MPa Case 1 : P = 13.8 kN = 0.65 P_{ult}

$f_{0.2}$ = 450 MPa Case P1 : P = 13.8 kN, ε_s^P = 5‰

$f_{0.2}^P$ = 1450 MPa Case P2 : P = 10.0 kN, ε_s^P = 5‰

ε_s^P = prestressing strain, A_s^P = prestressing steel area

Fig. 14 Characteristic data for three test examples, Case 1, P1 and P2

The initial moisture content in the concrete is taken as 3% by weight. The resulting emissivity at the concrete surfaces is set to 0.8, and the convection heat transfer coefficient is taken as 25W/m^2°C. Material properties according to Anderberg [3] and Harmathy & Stanzak [12] are assumed for the hot-rolled, reinforcing steel and the cold-drawn, prestressing steel ASTM A 421, respectively.

The predicted structural response of the plate strip in Case 1, P1 and P2 is shown in Fig. 15 in terms of mid-span deflection and stress in tensile reinforcement and prestressing steel, respectively. In the figure is indicated the fire resistance times if the failure criteria are based on max deflection $\delta = L/30$ (developed for standard fire resistance tests). If the failure criteria are based on strain limits (7‰ of concrete and 20‰ of steel), which is more consistant, the failure times are 82, 50 and 67 min for the cases 1, P1 and P2, respectively. For the cases P1 and P2 the failure is caused by very high creep.

Note that the steel stresses are lower at failure than at the beginning which is caused by a greater internal lever arm and a more concentrated compressive zone of concrete.

It is likely that somewhat higher fire resistance times in the cases P1 and P2 would have been obtained from the analysis if stabilized prestressing steel had been employed rather than the non-stabilized prestressing steel ASTM A 421. However, as indicated previously, relevant creep data are at present available only for ASTM 421.

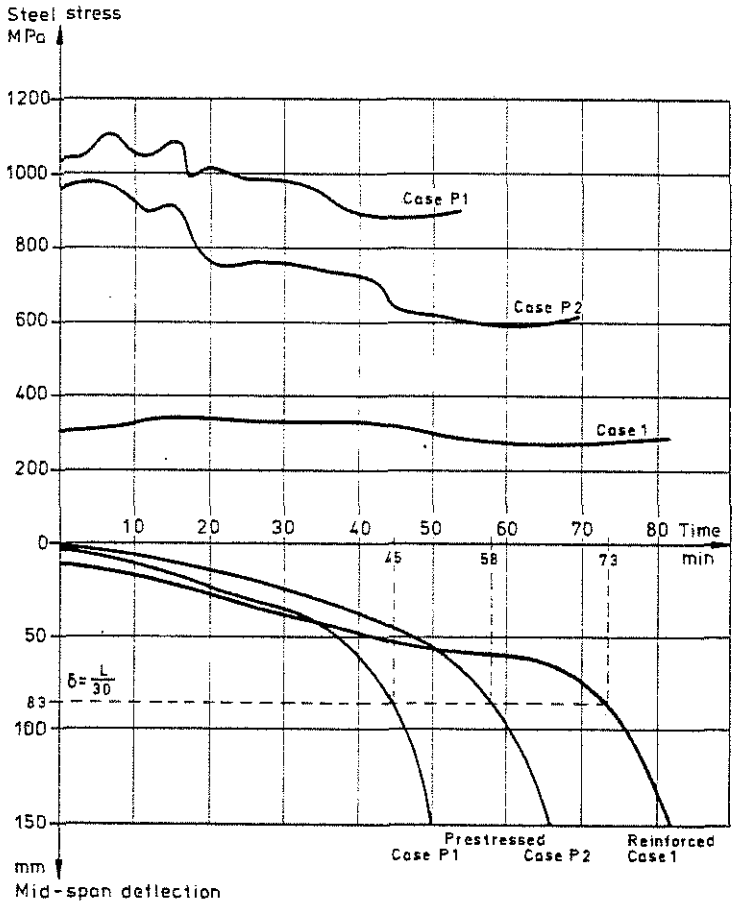

Fig. 15 Predicted structural behaviour of a fire-exposed plate strip in terms of mid-span deflection and steel stress. Data for the calculation are given in Fig. 14. Anderberg & Forsén (1983) [13]

3.2.2 Rotationally restrained

The plate strip described in Fig. 14 but totally restrained against rotation and free to move longitudinally is analysed. The structural behaviour in terms of restraint moment and mid-span deflections is computed with FIRES-RC and CONFIRE for comparison and checked against

experimental results (Fig. 16). The agreement is very good. Other comparisons have been made in [2].

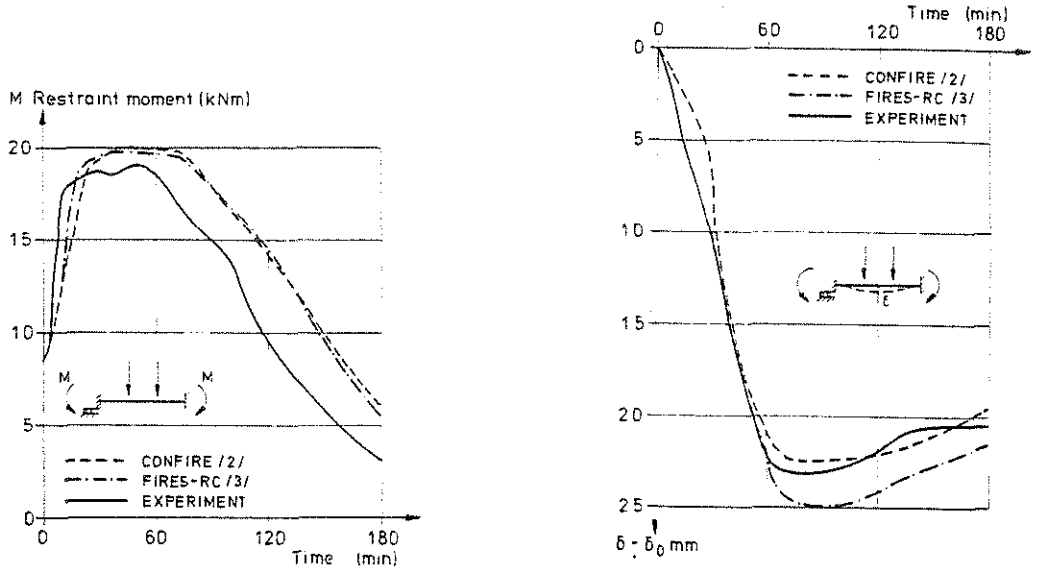

a) b)

Fig. 16 Measured and predicted results for test D20 [11]. Lateral twin load: 16 kN. Exposure according to simulated natural compartment fire
a) restraint moments
b) mid-span deflections

3.2.3 Axially restrained

It has been shown in tests on axially restrained, reinforced slabs and beams [14] that great axial forces may sometimes develop. Such axial restraint forces may increase the fire endurance significantly [15]. In [2] and [13] it is investigated if the thermal thrust, T, generally can be utilized in a fire design.

In the PCI-manual "Design for fire resistance of precast prestressed concrete", a calculation procedure is developed for determining the thermal thrust. The calculation is based on tests on a double T-unit of normal weight concrete and lightweight concrete. In the tests each specimen was permitted to expand to a given amount and further expansion was prevented. After expansion was stopped, the restraining force increased to a maximum value and then either diminished or remained relatively constant. Fig. 17 illustrates the maximum measured restraining forces for the prestressed specimens. It is significant that a small increase in expansion is accompanied by a large reduction in the restraining force.

The behaviour of the plate strip is predicted by CONFIRE in [2], [13] for different permissible expansions $\Delta L = 0$, 2, 4 and 6 mm at the center of gravity. The development of the axial force during a thermal exposure according to the ISO 834 standard fire resistance test is illustrated in Fig. 18. The second order effects are included in the full line curves but not in the dashed curves. The calculation illustrates the necessity to include the second order theory in the calculation. The full line curves, illustrate a structural behaviour which has not been possible to derive earlier. The thermal thrust attains a maximum value at an early stage, after the thrust has started to develop, and it then decreases rapidly and transfers into tension, if membrane forces can be taken at supports.

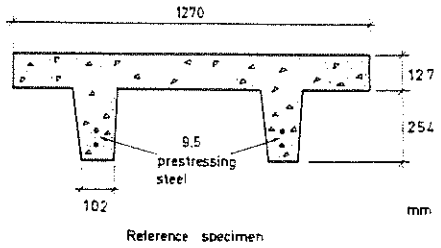

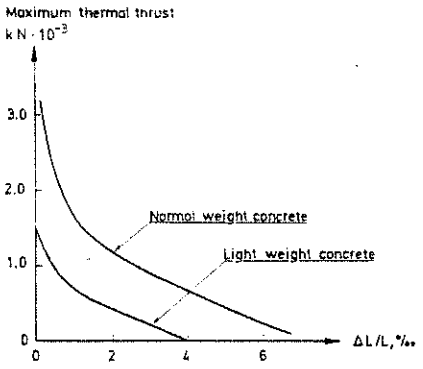

Fig. 17 Maximum restraining force measured during tests of reference specimens [15]

If membrane action is not possible, failure occurs when the thermal thrust has diminished to zero or possibly somewhat later.

The calculations show for all cases that without membrane action the failure time is much greater than the time at which maximum thrust occurs. This means that the maximum thrust for the plate strip studied cannot be utilized when calculating the fire resistance according to the PCI-manual. It must be emphasized that the development of restraint forces are very sensitive to the point of action of the cross-section.

If the maximum thermal thrust is calculated in accordance with the PCI-manual the curve shown in Fig. 19 is obtained. In the same figure the results are also given for the CONFIRE calculation. The difference between the curves is very obvious for $\Delta L/L > 0.15\%$. The conclusion from the analytical study is that the maximum thrust, acting at center of gravity, is smaller than according to the PCI-manual and at failure state, there is no longer any thrust.

The study illustrated here indicates that even if axial forces develop they may have no significant positive effect on the fire resistance. The point of action also ought to be considered. The PCI-calculation method, therefore, cannot be adopted generally. It can also be discussed if such a free elongation $\Delta L/L$, followed by a complete restraint, occurs in "real life". It should be more realistic to simulate different degrees of restraint defined by actual axial stiffness when studying thermal thrust.

Such a study is published in [2] and indicates positive effects on fire resistance if the point of action is below the center of gravity.

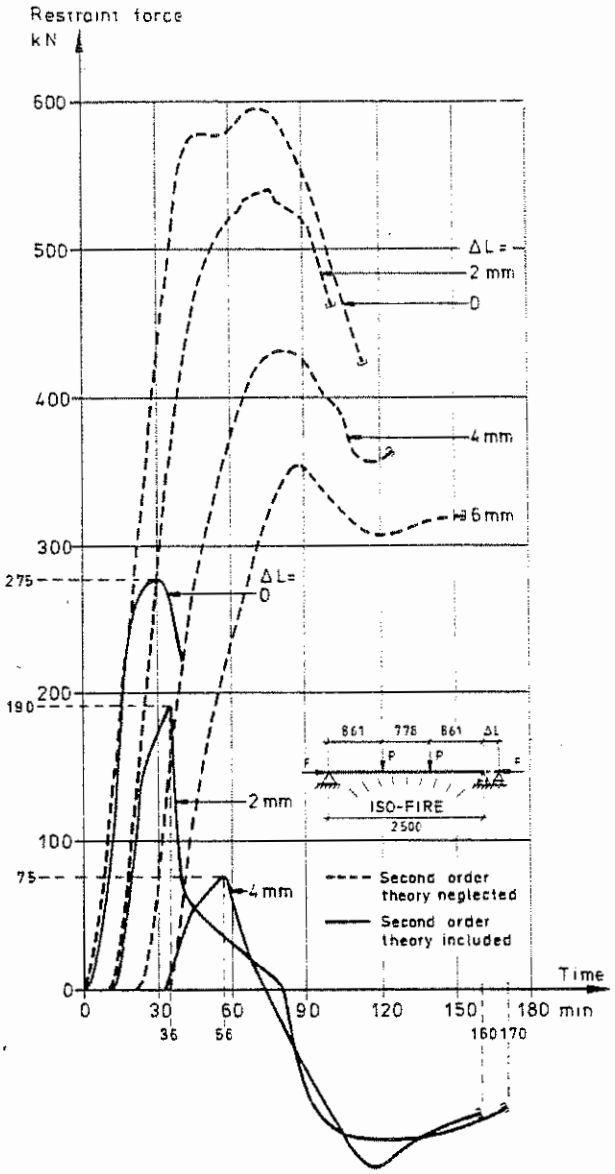

Fig. 18 Restraint forces for a fire-exposed reinforced plate strip (Case 1 as shown in Fig. 14) at different permissible expansions $\Delta L = 0, 2, 4$ and 6 mm and thereafter a complete restraint. Center of gravity is the point of action for restraint forces [2], [13]

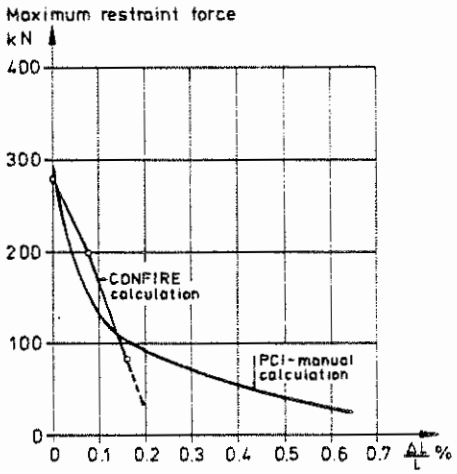

Fig. 19 Maximum restraining force as a function of permissible expansion $\Delta L/L$ for Case 1 (Fig. 14). A comparison between CONFIRE prediction and PCI-manual design calculation [13]

3.3 Fire-exposed columns

The program CONFIRE has also been used for verifying its reliability on two reinforced concrete columns exposed on three sides to ISO 834 standard fire [2], [13] and tested at the Swedish National Testing Institute in Borås. A similar theoretical study has been made in [16].

The predicted and measured temperatures are illustrated in Fig. 20. This figure gives the temperature of six points at the mid-section of the column as a function of time. The very good agreement obtained with TASEF-2 is significant and is earlier documented in [15]. Predicted temperatures are then inserted into CONFIRE structural program.

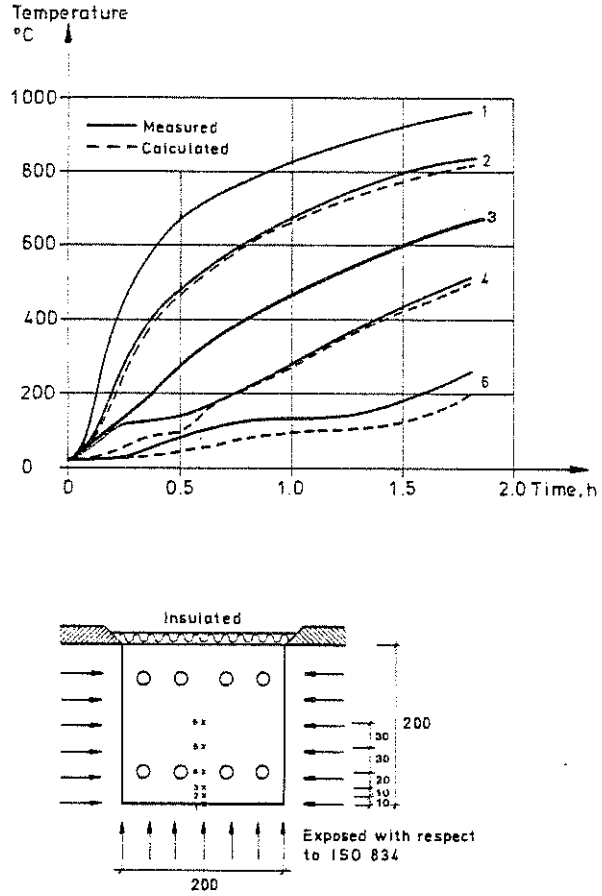

Fig. 20 Measured and calculated temperatures in the mid-section of the column

In the first study, the column is loaded to 0.6 MN with an eccentricity of 6 cm, directed from the furnace. The load corresponds to 63% of the ultimate load at normal conditions. In the test the measurements were stopped after 0.5 h due to a support failure, which was a mishap, but a comparison is still of interest. Fig. 21 illustrates mid-points deflection and axial elongation as a function of time obtained in test and calculation. The predicted deflection v, directed towards the furnace is in a very good agreement with the test but the axial elongation differs somewhat. The predicted and test estimated fire resistance are both about 0.7 h.

In the second comparison the same column was loaded to 0.3 MN with the same eccentricity but directed towards the furnace (see Fig. 22). This load corresponds to 31% of the original ultimate load. Both the predicted mid-point deflection, the axial movement and failure time

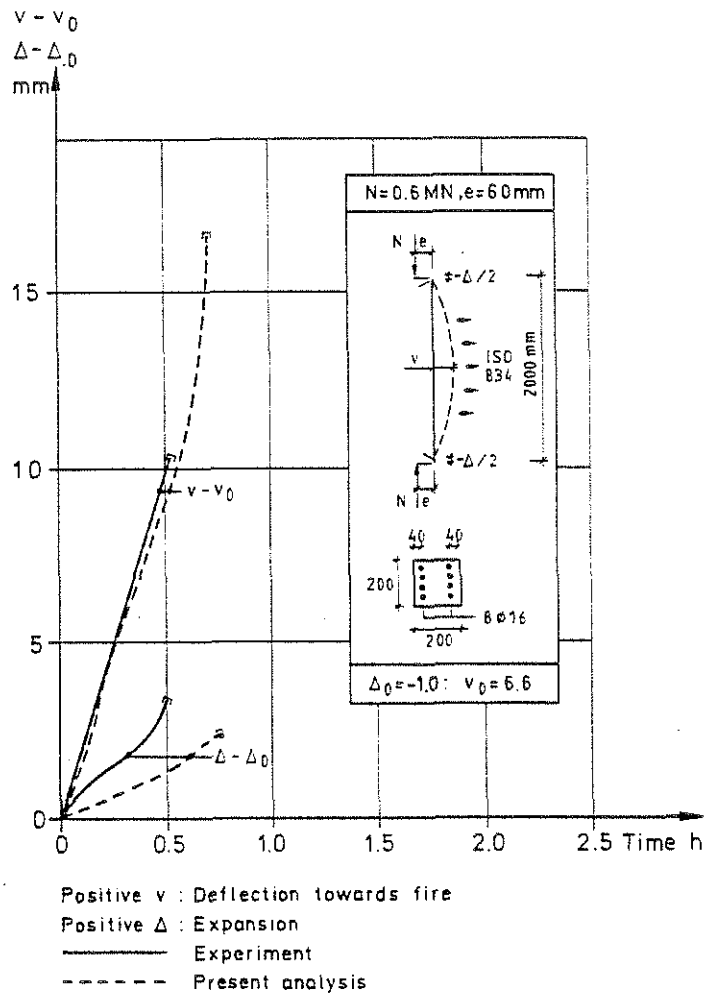

Fig. 21 Measured and calculated behaviour of a reinforced concrete column in a fire, eccentrically loaded to 0.6 MN

are in a quite good agreement with measured behaviour as shown in Fig. 22. It can be noted that the column expanded axially both in calculation and experiment during the first 1.7 h, but then it transferred into contraction in experiment. The sudden change into failure state is caused by a rapid inwards movement of the compression zone into the cross-section, which means that the tensile stress in the reinforcement increases to a critical value.

The two examples illustrate the reliability of TASEF-2 and CONFIRE computer programs.

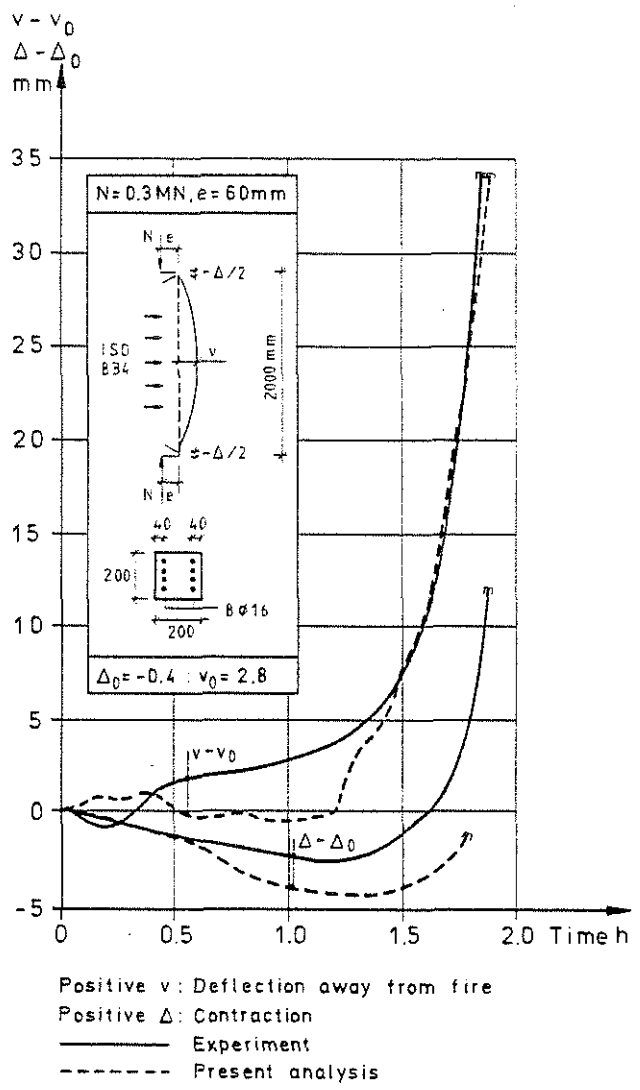

Fig. 22 Measured and calculated behaviour of a reinforced concrete column in a fire, eccentrically loaded to 0.3 MN

REFERENCES

1. ANDERBERG, Y. & THELANDERSSON, S. Stress Deformation Characteristics of Concrete at High Temperatures. 2. Experimental Investigation and Material Behaviour Model. Division of Structural Mechanics and Concrete Construction, Lund Institute of Technology. Bulletin 54, 1976. Lund.

2. FORSÉN, N.E. A Theoretical Study on the Fire Resistance of Concrete Structures. FCB-SINTEF, 1982. Trondheim.

3. ANDERBERG, Y. Fire-Exposed Hyperstatic Concrete Structures - An Experimental and Theoretical Study. Division of Structural Mechanics and Concrete Construction, Lund Institute of Technology. Bulletin 55, 1976. Lund.

4. DORN, J.E. Some Fundamental Experiments on High Temperature Creep. Journal of Mechanics and Physics of Solids 3(1954) 35. London.

5. ANDERBERG, Y. Mechanical Properties of Reinforcing Steel at Elevated Temperatures (Armeringsståls mekaniska egenskaper vid höga temperaturer). In Swedish with English summary. Tekniska Meddelanden Nr. 36, Halmstad Järnverk AB, 1978. Lund.

6. ANDERBERG, Y. Behaviour of Steel at High Temperatures. RILEM PHT-44, November 1982.

7. BECKER, J. & BRESLER, B. FIRES-RC, A Computer Program for the Fire Response of Structures - Reinforced Concrete Frames. University of California, Berkeley, Fire Research Group. Report No. UCB FRG 74-3, July 1974.

8. IDING, R., BRESLER, B. & NIZAMUDDIN, Z. FIRES-RC II, A Computer Program for the Fire Response of Structures - Reinforced Concrete Frames. Report No. UCB FRG 77-8. Fire Research Group, University of California, July 1977. Berkeley.

9. HAKSEVER, A. Zur Frage des Trag- und Verformungsverhaltens ebener Stahlbetonrahmen im Brandfall. Institut für Baustoffkunde und Stahlbetonbau der Technischen Universität Braunschweig. Heft 35, Mai 1977. Braunschweig.

10. WICKSTRÖM, U. TASEF-2 - A Computer Program for Temperature Analysis of Structures Exposed to Fire. Department of Structural Mechanics, Lund Institute of Technology. Report No. 79-2, 1979. Lund.

11. ÅLDSTEDT, E. Nonlinear Analysis of Reinforced Concrete Frames. Division of Structural Mechanics, Norwegian Institute of Technology. Report No. 75-1, March 1975. Trondheim.

12. HARMATHY, T. & STANZAK, W.W. Elevated Temperature Tensile and Creep Properties of Some Structural and Prestressing Steels. National Research Council of Canada. Research Paper No. 424, 1970. Ottawa.

13. ANDERBERG, Y. & FORSÉN, N.E. Fire Resistance of Concrete Structures. Nordic Concrete Research No. 1, 1983.

14. ISSEN, L.A., GUSTAFERRO, A.H. & CARLSON, C.C. Fire Tests on Concrete Members: An Improved Method for Estimating Thermal Restraint Forces, Fire Test Performance. ASTM, STP 464. American Society for Testing and Materials, 1970, pp. 153-185.

15. PCI-manual. Design for Fire Resistance of Precast Prestressed Concrete, 1977.

16. ANDERBERG, Y. & HAKSEVER, A. Comparison between Measured and Computed Structural Response of Some Reinforced Concrete Columns in Fire. Fire Safety Journal 4(1981/82) 293-297. Lund Institute of Technology and Technical University Braunschweig.

APPENDIX

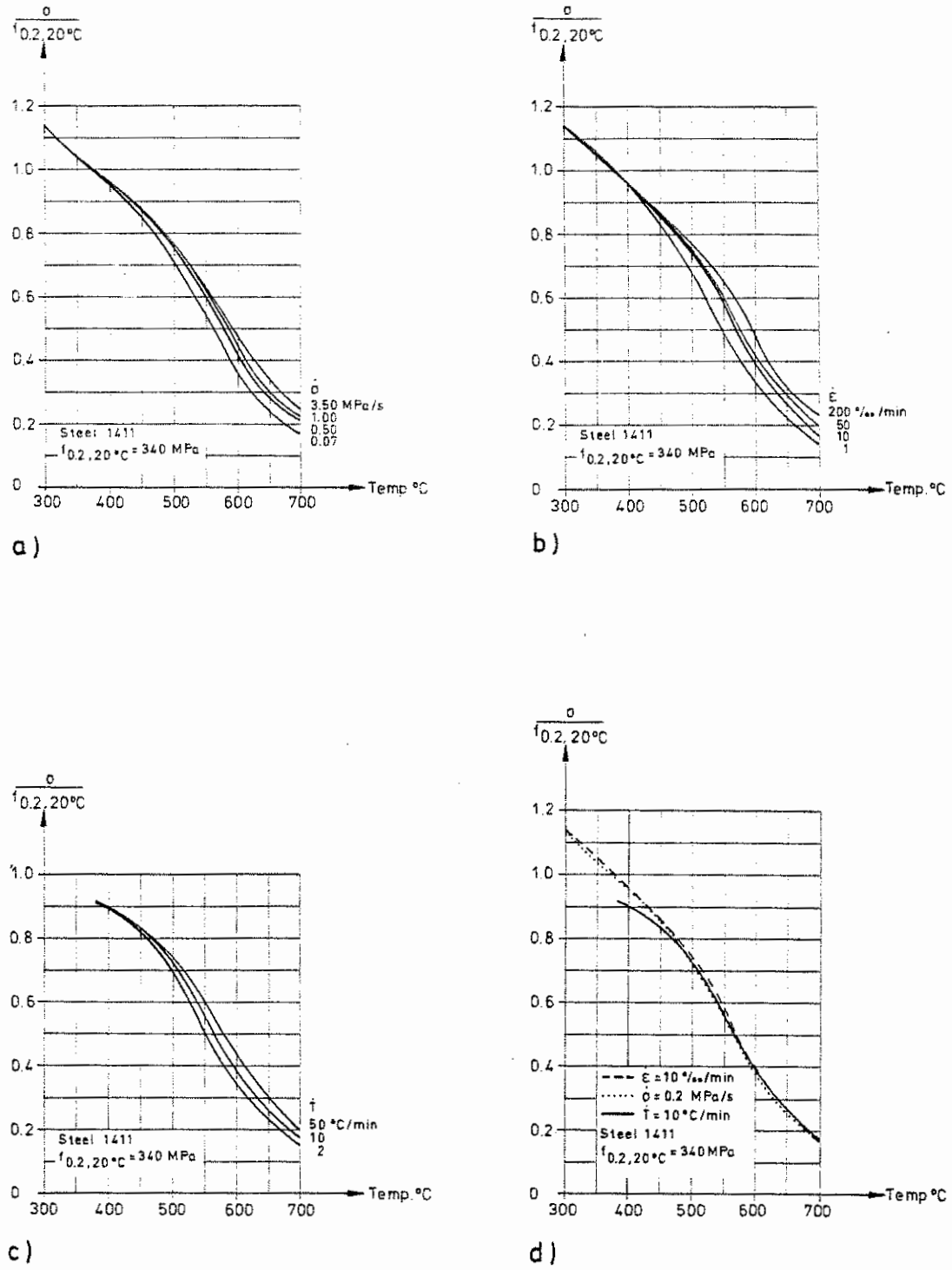

Fig. A1 Predicted ultimate strength versus temperature for reinforcing steel
a) steady state, stress rate controlled
b) steady state, strain rate controlled
c) transient state
d) comparison between steady state and transient state

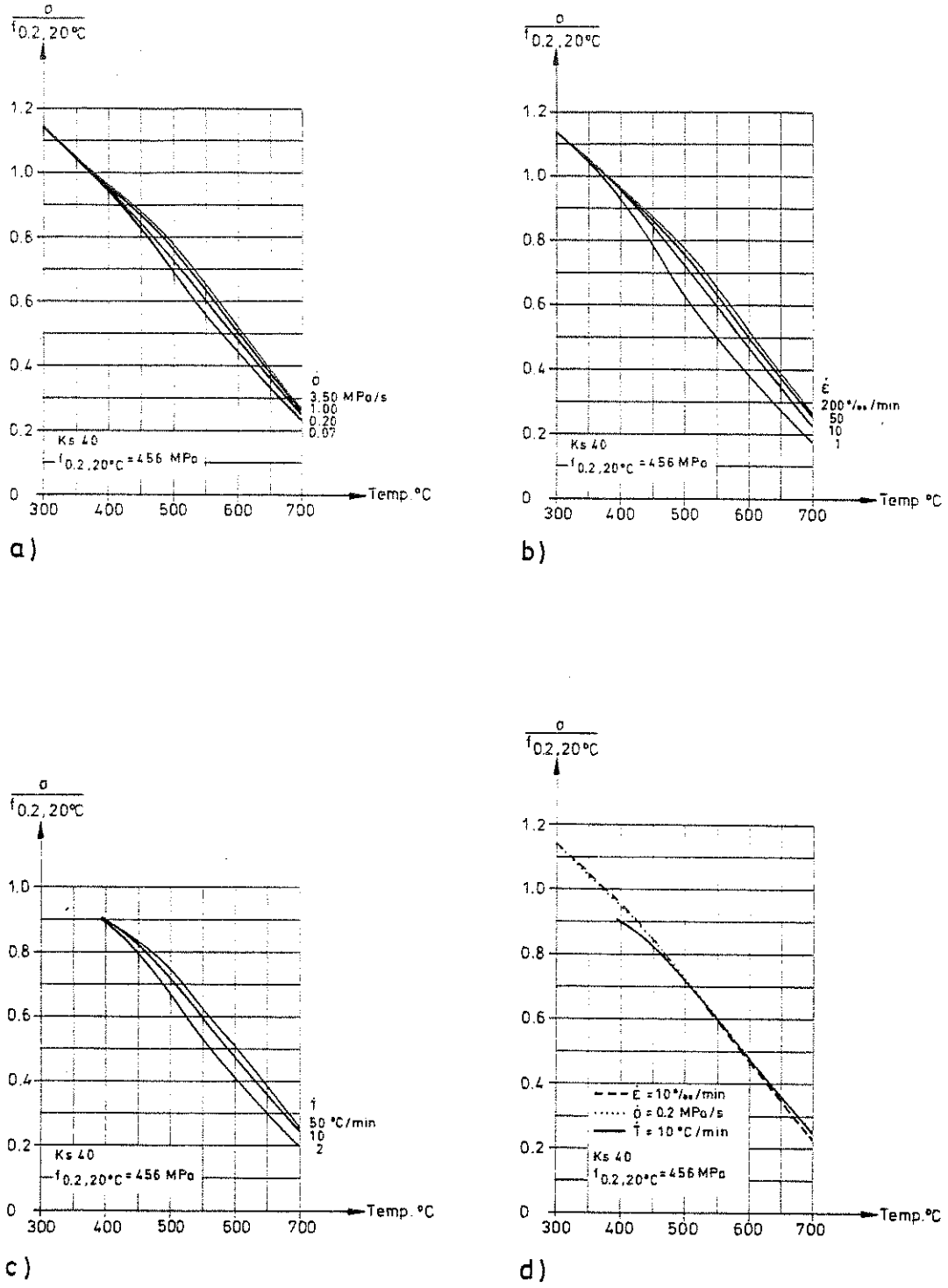

Fig. A2 Predicted ultimate strength versus temperature for reinforcing steel Ks 40
a) steady state, stressrate controlled
b) steady state, strainrate controlled
c) transient state
d) comparison between steady state and transient state

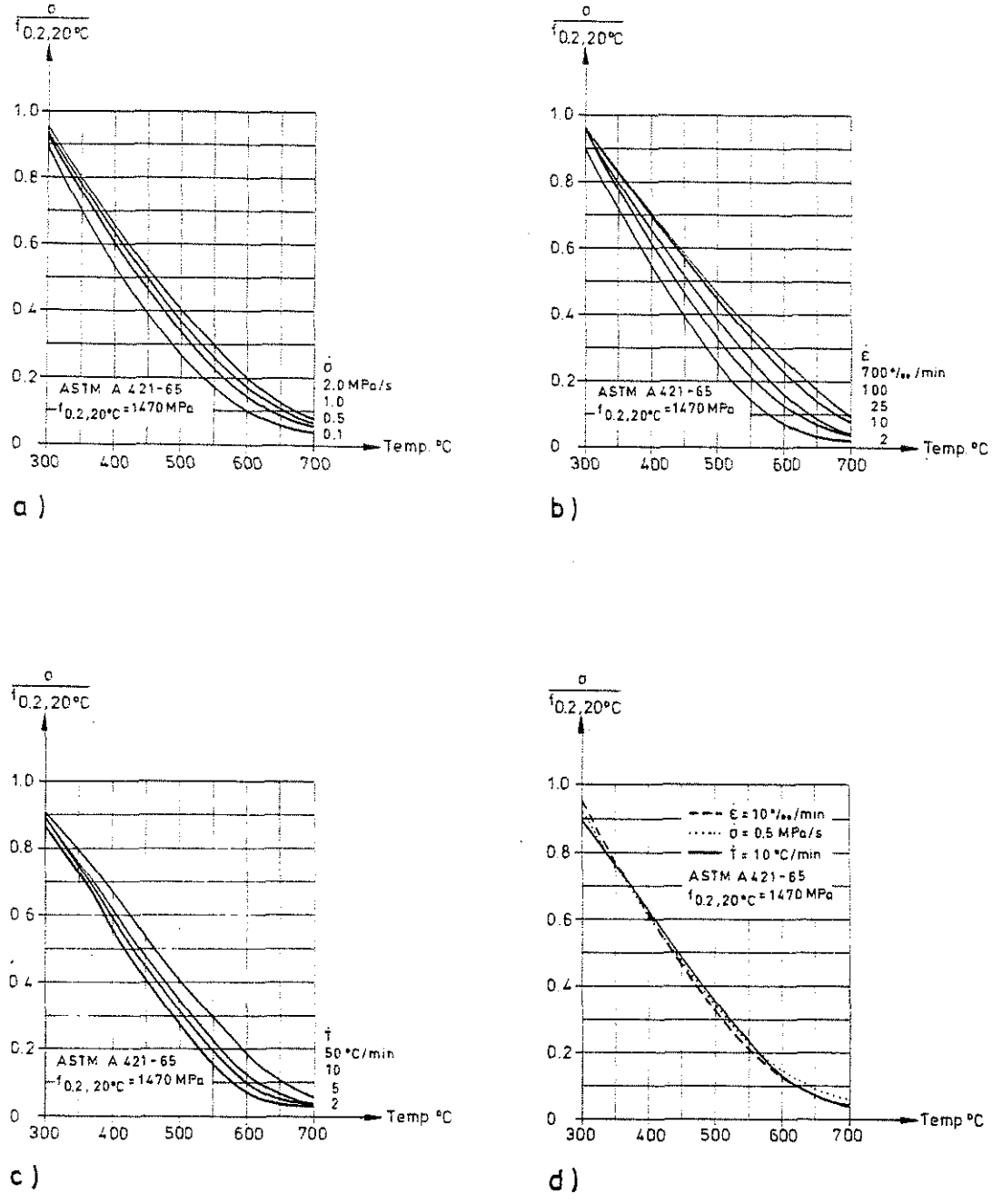

Fig. A3 Predicted ultimate strength versus temperature for prestressing steel ASTM 421-65

a) steady state, stressrate controlled
b) steady state, strainrate controlled
c) transient state
d) comparison between steady state and transient state